Assessment of ENDF/B-VIII.0 and TENDL-2015 Evaluated Nuclear Data Libraries Using Stellar Nucleosynthesis Modeling

Boris Pritychenko[1]

1 National Nuclear Data Center, Brookhaven National Laboratory, Upton, NY 11973-5000, USA

BROOKHAVEN NATIONAL LABORATORY

U.S. DEPARTMENT OF ENERGY

Stellar Nucleosynthesis Observables

- Stellar nucleosynthesis manifest itself by the present variety of elements and isotopes.
- ^{56}Fe has the highest binding energy per nucleon, and it is very common in the Earth's crust.
- For nuclei lighter than ^{56}Fe fusion is preferable and fission for heavier.
- Stellar nucleosynthesis: Big Bang, explosive burning, *s*-, *r*- and *rp*- processes (slow and rapid neutron capture).
- Most of the stable nuclei in ^{56}Fe-^{210}Po range are produced by the *s*-process and (*s*+*r*).
- Very neutron rich and actinide nuclides are produced by *r*-process.

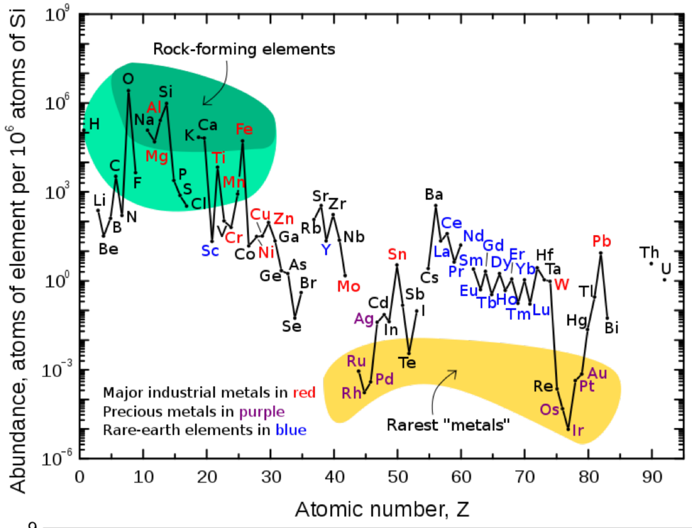

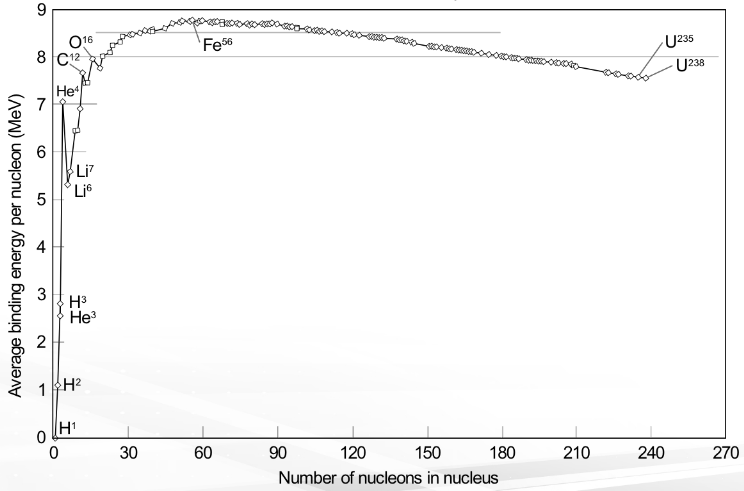

Slow Neutron Capture, *s*-process

- Takes place in AGB or Red Giants stars.
- It is all about neutron capture, neutron magic numbers and β-decays along the valley of stability in nuclear chart.
- *s*-process golden rules:
  - Neutron closed shell (N=50, 82, 126) nuclei have low neutron-capture cross sections, and they act as bottlenecks.
  - In-between neutron bottlenecks the abundances are in equilibrium.
  - Branching points may occur on the s-process path when β-decay rate competes with neutron capture.

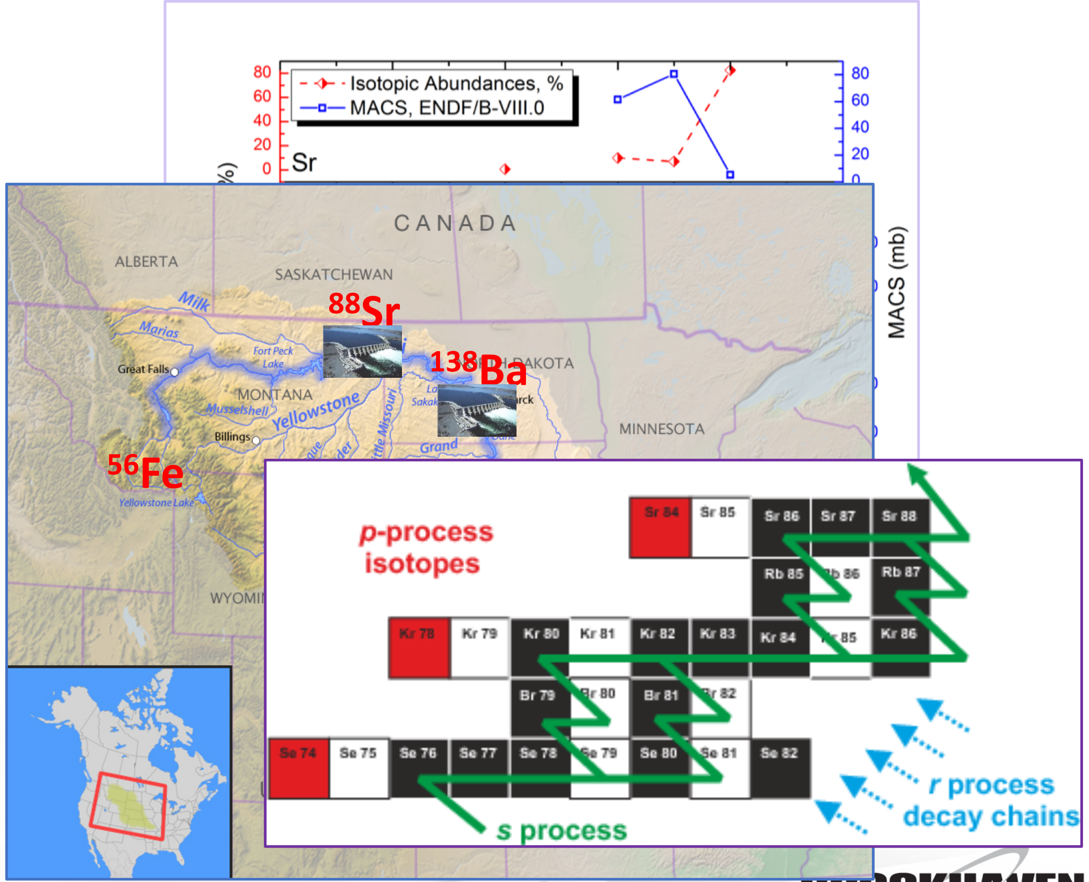

ENDF & Slow Neutron Capture

- ENDF neutron materials list matches well with an *s*-process path.
- Slow neutron capture Maxwellian-averaged cross sections (MACS) can be expressed as

$$\sigma^{Maxw}(kT) = \frac{2}{\sqrt{\pi}} \frac{(m_1/(m_1+m_2))^2}{(kT)^2} \int_0^\infty \sigma(E_n^L) E_n^L \exp\left(-\frac{aE_n^L}{kT}\right) dE_n^L$$

where *k* and *T* are the Boltzmann constant and temperature of the system, respectively, and E is an energy of relative motion of the neutron with respect to the target. Here E^L_n is a neutron energy in the laboratory system and m_1 and m_2 are masses of a neutron and target nucleus.

- We can calculate MACS and astrophysical reaction rates by Doppler broadening cross sections and numerical integration.

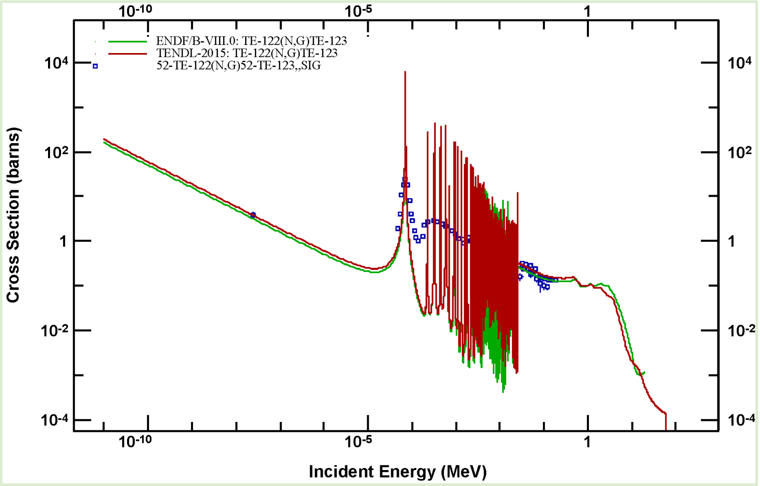

Data for Stellar Nucleosynthesis

- In the recent years CSEWG collaboration has released ENDF/B-VII.0, ENDF/B-VII.1 and ENDF/B-VIII.0 evaluated nuclear data libraries.
- They are widely used in nuclear energy, national security appilactions, MCNP and GEANT codes. Why not in nuclear astophysics where people rely on narrow-defined data colections like KADoNiS?
- Maxwellian-averaged cross sections (MACS) for slow neutron capture (*s*) process:
    - ENDF/B-VII.0 MACS & Reaction Rates: ADNDT 96, 645 (2010).
    - ENDF/B-VII.1 MACS & Reaction Rates with Uncertainties: NDS 113, 3120 (2012).
    - ENDF/B-VIII.0 MACS with Uncertainties: NDS 148, 1 (2018).

ELSEVIER

Atomic Data and Nuclear Data Tables

Volume 96, Issue 6, November 2010, Pages 645-748

Calculations of Maxwellian-averaged cross sections and astrophysical reaction rates using the ENDF/B-VII.0, JEFF-3.1, JENDL-3.3, and ENDF/B-VI.8 evaluated nuclear reaction data libraries

B. Pritychenko, S.F. Mughaghab, A.A. Sonzogni

Show more

ELSEVIER

Nuclear Data Sheets

Volume 113, Issue 12, December 2012, Pages 3120-3144

Neutron Thermal Cross Sections, Westcott Factors, Resonance Integrals, Maxwellian Averaged Cross Sections and Astrophysical Reaction Rates Calculated from the ENDF/B-VII.1, JEFF-3.1.2, JENDL-4.0, ROSFOND-2010, CENDL-3.1 and EAF-2010 Evaluated Data Libraries

B. Pritychenko [a], S.F. Mughabghab [a]

ELSEVIER

Nuclear Data Sheets

Volume 148, February 2018, Pages 1-142

ENDF/B-VIII.0: The 8th Major Release of the Nuclear Reaction Data Library with CIELO-project Cross Sections, New Standards and Thermal Scattering Data

D.A. Brown [a], M.B. Chadwick [b], R. Capote [c], A.C. Kahler [b], A. Trkov [c], M.W. Herman [a], A.A. Sonzogni [a], Y. Danon [d], A.D. Carlson [e], M. Dunn [f], D.L. Smith [g], G.M. Hale [b], G. Arbanas [h], R. Arcilla [a], C.R. Bates [b], B. Beck [i], B. Becker [j], F. Brown [b], R.J. Casperson [i], J. Conlin [b], D.E. Cullen [i], M.-A. Descalle [i], R. Firestone [k], T. Gaines [l], K.H. Guber [h], A.I. Hawari [m], J. Holmes [n], T.D. Johnson [a], T. Kawano [b], B.C. Kiedrowski [o], A.J. Koning [c], S. Kopecky [p], L. Leal [q], J.P. Lestone [b], C. Lubitz [r], J.I. Márquez Damián [s], C.M. Mattoon [i], E.A. McCutchan [a], S. Mughabghab [a], P. Navratil [t], D. Neudecker [b], G.P.A. Nobre [a], G. Noguere [u], M. Paris [b], M.T. Pigni [h], A.J. Plompen [p], B. Pritychenko [a], V.G. Pronyaev [v], D. Roubtsov [w], D. Rochman [x], P. Romano [g], P. Schillebeeckx [p], S. Simakov [y], M. Sin [z], I. Sirakov [aa], B. Sleaford [i], V. Sobes [h], E.S. Soukhovitskii [ab], I. Stetcu [b], P. Talou [b], I. Thompson [i], S. van der Marck [ac], L. Welser-Sherrill [b], D. Wiarda [h], M. White [b], J.L. Wormald [m], R.Q. Wright [h], M. Zerkle [n], G. Žerovnik [p], Y. Zhu [m]

First test: *s*-process Time Scale Estimates

- In the classical model we assume that neutron temperature (*kT*) and density stay constant during the nucleosynthesis.
- To verify this assumption *s*-process we calculate time scale (τ_n) using neutron density of $N_n=10^8$ n/cm^3 that is within a typical *s*-process range of 10^7-10^{11} n/cm^3:

$$\tau_n = \sum_{i=56}^{209} \frac{1}{N_n \langle \sigma_i v_i \rangle},$$

where $R(T_9)/N_A = \langle \sigma v \rangle$ is astrophysical reaction rate.

- The obtained values could be compared with an AGB star lifetime of about one million years.
- *s*-process takes less than 1% of the star lifetime, and it is sensitive to magic nuclei cross sections (^{208}Pb,^{209}Bi where MACS can be deficient).

Table 2: s-process lifetime scale estimates for ENDF/B-VIII.0, TENDL-2015 and KADoNiS libraries [5, 6, 10].

s-process	ENDF/B-VIII.0	TENDL-2015	KADoNiS
Complete (y)	5.229E+3	5.344E+3	6.993E+3
Excluding ^{208}Pb, ^{209}Bi (y	2.721E+3	2.730E+3	2.717E+3

ENDF Validation: *s*-process Modeling

- The *s* -process abundance of an isotope $N_{(A)}$ depends on its precursor $N_{(A-1)}$ quantity as: $dN_{(A)}/dt=\sigma_{(A-1)}N_{(A-1)}+\sigma_{(A)}N_{(A)}$ *(5)*

The equation 5 was solved analytically by Clayton & Ward (Clayton & Ward 1974) for an exponential average flow of neutron exposure assuming that temperature remains constant over the whole time scale of the s-process, and the product of MACS and isotopic abundance ($\sigma_{(A)}N_{(A)}$) was deduced as

$$\sigma_{(A)}N_{(A)} = \frac{fN_{56}}{\tau_0}\prod_{i=56}^{A}[1+\frac{1}{\sigma(i)\tau_0}]^{-1}, \quad (6)$$

where f and τ_0 are neutron fluence distribution parameters, and N_{56} is the initial abundance of ^{56}Fe seed. Finally, at the s-process equilibrium, the equation 5 becomes

$$\sigma_{(A-1)}N_{(A-1)} = \sigma_{(A)}N_{(A)} = constant. \quad (7)$$

- Next, we select *s*-process only nuclides along the *s*-process path and fit present-day MACS abundance product values with Formula 6 using least squares.
- Fitting parameters allow to calculate expected s-process contributions and compare with the presently-observed product values.
- The observed surplus is commonly attributed to an *r*-process (rapid neutron capture) contribution, and it can be deduced by subtracting the *s*-process input from the neutron capture MACS Anders & Greevese solar system abundances product, and dividing the remainder by evaluated MACS.

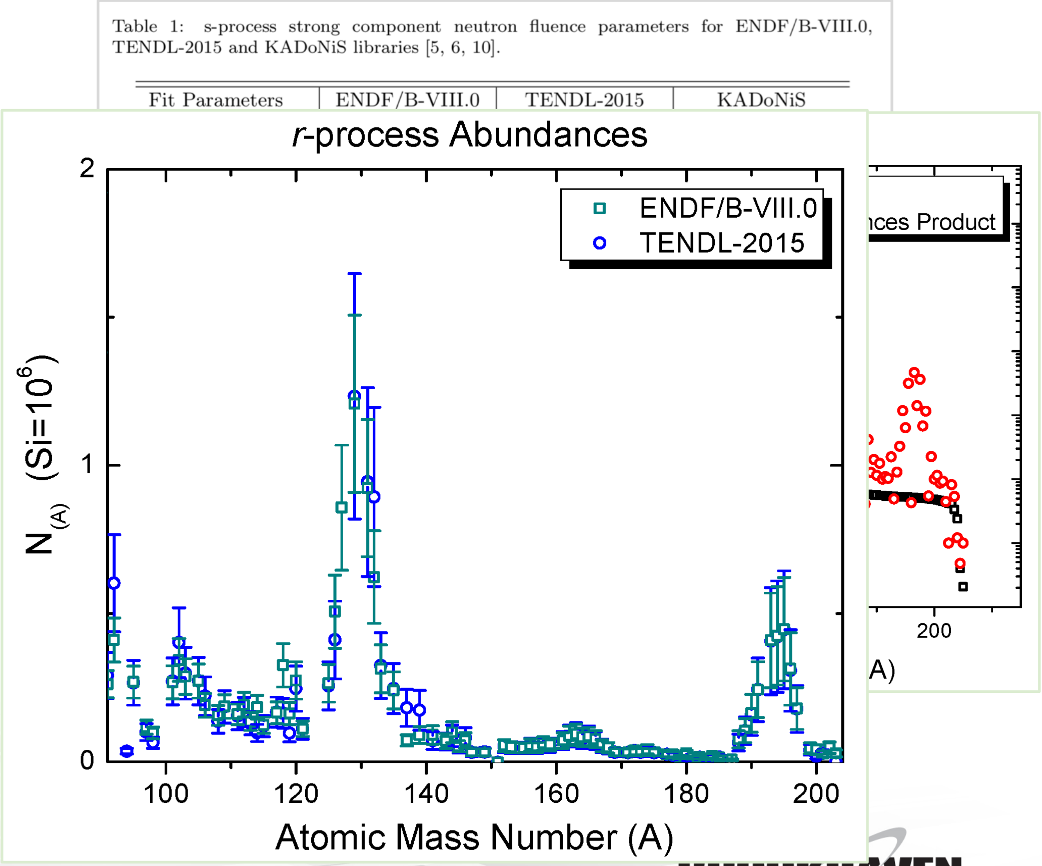

Heavy Elements Production in a Neutron Star Merger

- Can we apply nuclear data libraries to address current astrophysical observations such as a multi-messenger signal from the NGC 4993 galaxy?
- GW170817 was a gravitational wave signal observed by the LIGO and Virgo detectors on 17 August 2017; plus EM signal.
- The rapid-neutron capture (*r*) process element production was tentatively observed.
- The Doppler-shifted ejecta optical spectra consistent with Lanthanide and heavy elements.
- The *r*-process abundances can be deduced from evaluated neutron cross sections and solar system element abundances.
- Courtesy of NASA (Unique Gamma-Ray Burst): *https://www.nasa.gov/vision/universe/watchtheskies/short_burst.html*.

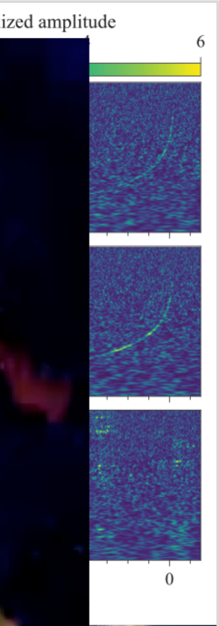

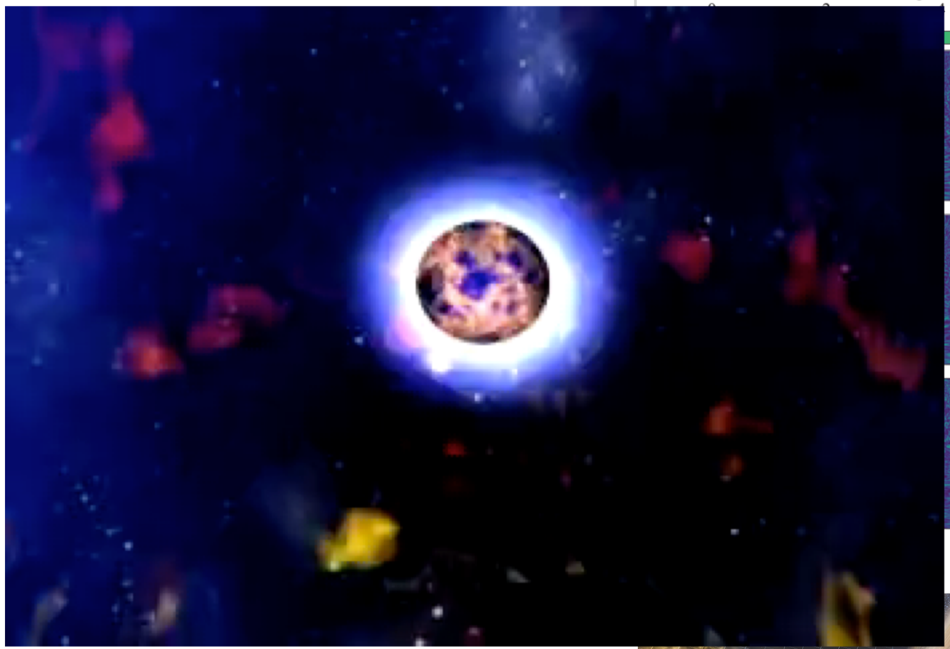

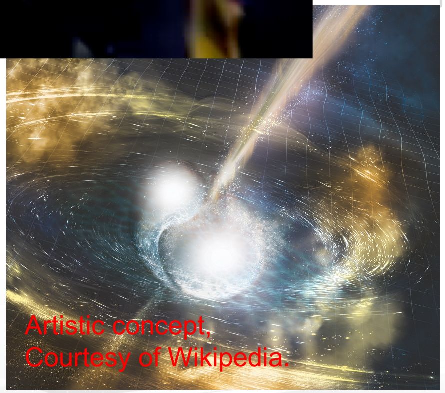

Artistic concept,
Courtesy of Wikipedia.

Comparison with Others

- Several *r*-process calculations produced isotopic abundances.
- Multi-event model results of *M. Arnould et al., Phys. Rep. 450, 97 (2007)*.
- Classical model based on ENDF/B-VIII.0 cross sections and Anders & Greevese solar system abundances agrees with the multi-event model predictions.
- The ratio of ENDF/B-VIII.0 and Arnould et al (2007) provides information on potential deficiencies, possible ENDF library improvements.
- Next stage (in progress), it would be necessary to calculate ENDF/B-VIII.0 & TENDL-2015 reaction rates, fit data into REACLIB (astrophysical data format) and start a new round of testing with codes like MESA….

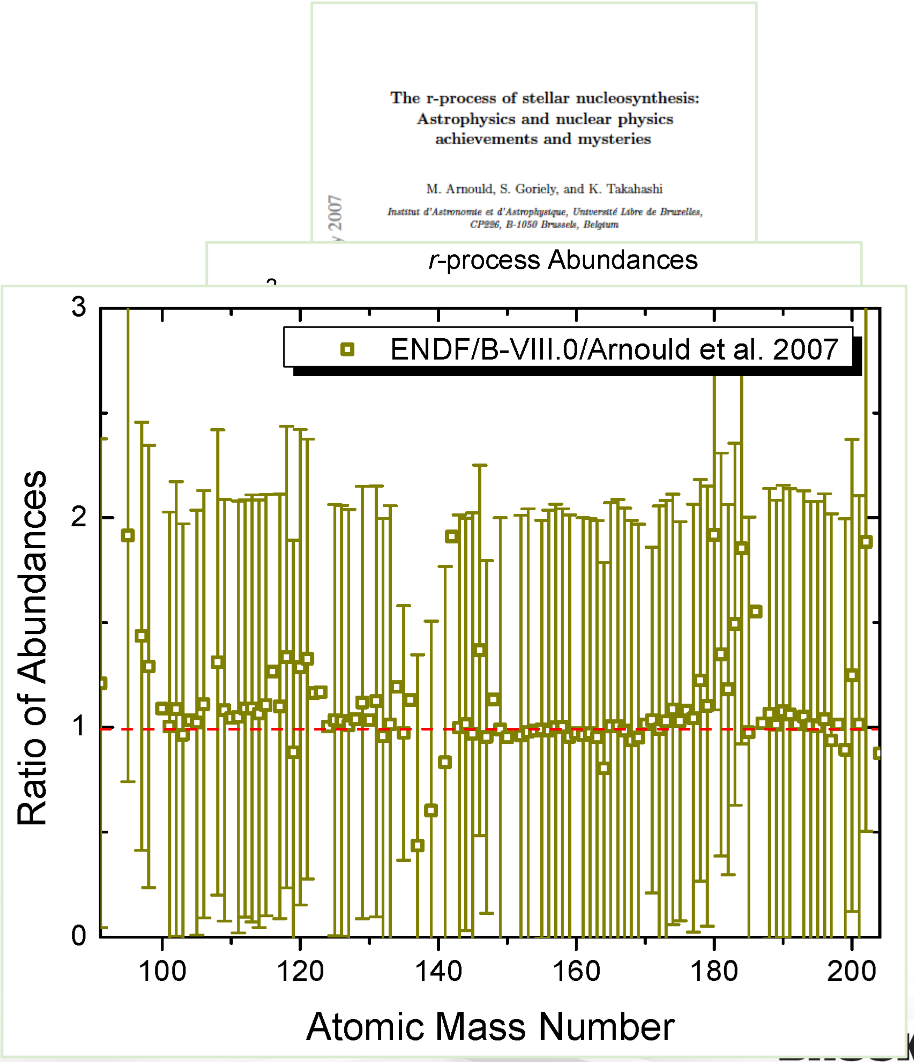

ENDF/B-VIII.0 & M. Arnould et al. 2007

- Documentation multi-event model vs. ENDF procedures: ENDF/B-VIII.0 is clearly better documented.
- Deviations are within error bars except ^{92}Zr and ^{203}Tl:
  - ^{137}Ba, ^{139}La, ^{141}Pr higher *r*-process abundances in Arnould.
  - ^{92}Zr, ^{95}Mo, ^{118,120}Sn, ^{121}Sb, ^{146}Nd, ^{178,180}Hf, ^{181}Ta, ^{183,184}W, ^{203}Tl lower *r*-process abundances in Arnould.
  - *s*-process overproduction (lower in Arnould): ^{202}Hg.
  - Pure r-process abundances differences between experimental compilation of Anders & Greevese and theoretical calculation of Arnould et al.: ^{116}Cd, ^{122}Sn, ^{123}Sb, ^{142}Ce, ^{186}W.
  - ^{88}Sr, ^{138}Ba, ^{140}Ce negative ratios will be discussed later.
- Work on tracing the differences is in progress.

ENDF/B-VIII.0 & KADoNiS

- Multiple changes to ENDF/B-VIII.0 library compare to ENDF/B-VII.1.
- ^{141}Pr, ^{121}Sb, ^{178}Hf MACS agree with KADoNiS.
- ^{92}Zr, ^{95}Mo, ^{118,120}Sn (small difference), ^{139}La, ^{146}Nd, ^{181}Ta, ^{183,184}W, ^{202}Hg, ^{203}Tl MACS are lower in ENDF/B-VII.1 compare to KADoNiS.
- ^{137}Ba, ^{88}Sr, ^{140}Ce and ^{138}Ba (small difference) MACS are higher in ENDF/B-VIII.0 compare to KADoNiS.
- ^{137}Ba is difficult to judge, while ^{88}Sr, ^{140}Ce and ^{138}Ba more interesting.
- Finally, 63 target nuclei (^{103}Rh-^{197}Au) have been updated in KADoNiS recently using the ENDF recommendations from Dr. A. Carlson, see **2018RE13**. This update makes the current analysis obsolete.
- Interesting finding, **1996KA03** is missing in EXFOR (Area #2), and asked NEA-DB to compile it. Ce was measured relative to gold, corrections are needed. ENSDF evaluators would not allow such situation, while ENDF relies on X4 or X4toC4??

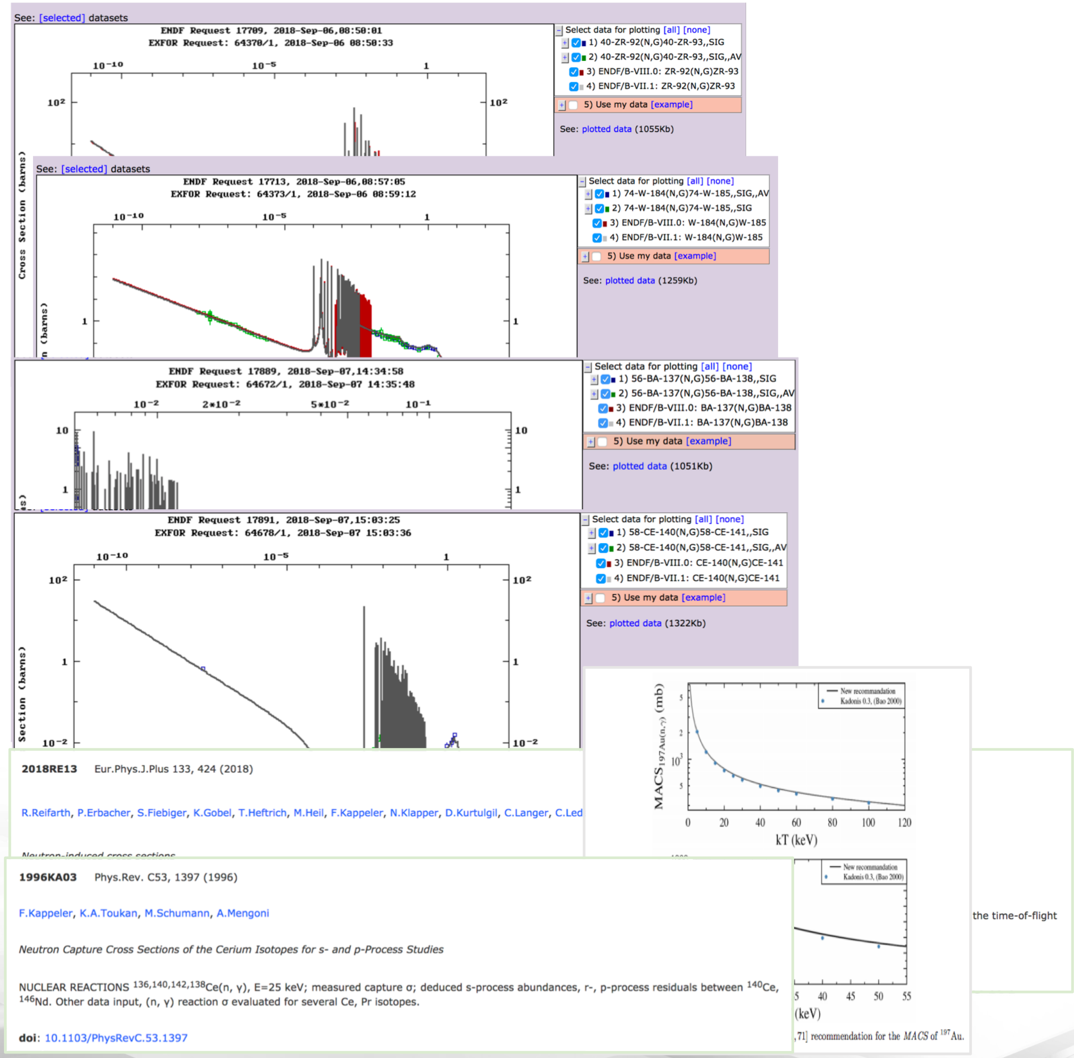

Potential ENDF Library Deficiencies

- First, we have to verify ^{208}Pb and ^{209}Bi cross sections in ENDF and TENDL libraries.
- ^{76}Se(n,γ) cross section is important for massive stars but Viktor's interface fails to show data coded as *kT*=30 keV instead of E.
- Probable issues with ^{116}Sn,^{122}Te(n,γ) *s*-process model fitting (non flat) in ENDF and ^{116}Sn, ^{123,124}Te (n,γ) in TENDL.
- ^{88}Sr (*N=50*), ^{138}Ba and ^{140}Ce (*N=82*) capture cross section abundance products are lower than *s*-process only predictions for ENDF/TENDL result in negative *r*-process abundances:
    - Wrong cross section/ resonance parameters values in "SG23: International library of fission product evaluations".
    - Wrong abundances for ^{88}Sr, ^{138}Ba and ^{140}Ce in Anders & Greevese's compilation.
    - *s*-process overproduction of ^{138}Ba and ^{88}Sr?????
- The similar negative *r*-process abundance values for ^{127}I,^{202}Hg,^{203}Tl in TENDL-2015.
- Practical nucleosynthesis network coverage in ENDF/B-VIII.0:
    - We have only ^{197}Au, no ^{198}Au ($T_{1/2}$=2.7 d) in ENDF/B-VIII.0.
    - Po… Ra gap, why no calculated values for α-decaying nuclides?

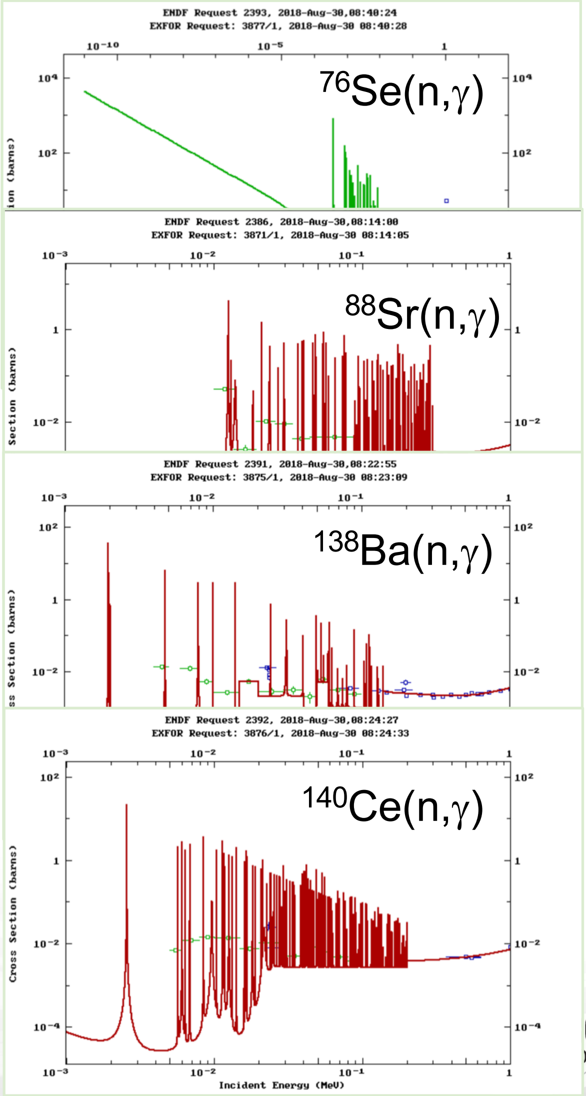

Conclusions & Outlook

- The recent releases of the ENDF/B-VIII.0 and TENDL-2015 libraries provide a unique opportunity to apply these data for astrophysical applications.
- GW170817 neutron star merger renewed interest in stellar nucleosynthesis calculations.
- This astrophysical event is timely-matched with the ENDF/B-VIII.0 library release.
- *r*-process abundances have been calculated using ENDF/B-VIII.0 and TENDL-2015 evaluated neutron cross sections and Anders & Greevese solar system abundances.
- These results have been compared with a multi-event model of of *M. Arnould et al., Phys. Rep. 450, 97 (2007)*, and the agreement is good.
- The *s*-process timescales have been estimated for ENDF/B-VIII.0, TENDL-2015 and KADoNiS library reaction rates.
- Several potential deficiencies in ENDF/B-VIII.0 and TENDL-2015 libraries were found, and recommendations for future releases were produced.
- Current work involves fitting of ENDF reaction rates, production of REACLIB files and future testing/computations with nuclear astrophysics codes.